

A COMPARISON OF OBSERVATIONALLY DETERMINED RADII WITH THEORETICAL RADIUS PREDICTIONS FOR SHORT-PERIOD TRANSITING EXTRASOLAR PLANETS

GREGORY LAUGHLIN,¹ AARON WOLF,¹ TONNY VANMUNSTER,² PETER BODENHEIMER,¹
DEBRA FISCHER,³ GEOFF MARCY,⁴ PAUL BUTLER,⁵ AND STEVE VOGT¹

Received 2004 October 27; accepted 2004 November 17

ABSTRACT

Two extrasolar planets, HD 209458b and TrES-1, are currently known to transit bright parent stars for which physical properties can be accurately determined. The two transiting planets have very similar masses and periods and hence invite detailed comparisons between their observed and theoretically predicted properties. In this paper, we carry out these comparisons. We first report photometric and spectroscopic follow-up observations of TrES-1, and we use these observations to obtain improved estimates for the planetary radius, $R_{\text{pl}} = (1.08 \pm 0.05)R_J$, and the planetary mass, $M_{\text{pl}} = (0.729 \pm 0.036)M_J$. We also confirm that the inclination estimate of the planetary orbit as $i = 88^\circ 2$. These values agree with those obtained by Alonso et al. in their discovery paper, but the uncertainty in the planet radius has been improved as a result of both high-cadence photometry of two full transits and from independent radius determinations for the $V = 11.8$ K0 V parent star. We derive estimates for the TrES-1 stellar parameters of $R_*/R_\odot = 0.83 \pm 0.03$ (by combining independent estimates from stellar models, high-resolution spectra, and transit light curve fitting) $M_*/M_\odot = 0.87 \pm 0.05$ (via fitting to evolutionary tracks), $T_{\text{eff}} = 5214 \pm 23$ K, $[\text{Me}/\text{H}] = 0.001 \pm 0.04$, rotational velocity $V \sin(i) = 1.08 \pm 0.3$ km s⁻¹, $\log g = 4.52 \pm 0.05$ dex, $\log L_*/L_\odot = -0.32$, $d = 157 \pm 6$ pc, and an age of $\tau = 4 \pm 2$ Gyr. These estimates of the physical properties of the system allow us to compute evolutionary models for the planet that result in a predicted radius of $R_{\text{pl}} = 1.05R_J$ for a model that contains an incompressible $20 M_\oplus$ core and a radius $R_{\text{pl}} = 1.09R_J$ for a model without a core. We use our grids of planetary evolution models to show that, with standard assumptions, our code also obtains good agreement with the observed radii of the other recently discovered transiting planets, including OGLE-TR-56b, OGLE-TR-111b, OGLE-TR-113b, and OGLE-TR-132b. We report an updated radius for HD 209458b of $R_{\text{pl}} = (1.32 \pm 0.05)R_J$, based on a new radius estimate of $R_* = 1.12 R_\odot$ for the parent star. Our theoretical predictions for the radius of HD 209458b are $R_{\text{pl}} = 1.05R_J$ and $1.09R_J$ for models with and without cores. HD 209458b is therefore the only transiting planet whose radius does not agree well with our theoretical models. We argue that tidal heating stemming from dynamical interaction with a second planet is currently the most viable explanation for its inflated size.

Subject headings: planetary systems — planets and satellites: general — stars: individual (HD 209458, TrES-1)

1. INTRODUCTION

The discovery of the transiting planet HD 209458b (Charbonneau et al. 2000; Henry et al. 2000) is still reverberating through the astronomical community. The intense interest in the HD 209458b detection results in no small part from HD 209458 itself being bright enough ($V = 7.68$) to allow a plethora of high-precision follow-up measurements of both the planetary and the stellar characteristics.

From a theoretical standpoint, the most important properties that one can derive from a combination of transit photometry and radial velocity measurements are the mass M_{pl} and the radius R_{pl} of the planet. For HD 209458b, current radius estimates in the literature are $R_{\text{pl}} = (1.35 \pm 0.06)R_J$ by Brown et al. (2001) and $R_{\text{pl}} = (1.41 \pm 0.10)R_J$ by Cody & Sasselov (2002), whereas the mass is estimated to be $M_{\text{pl}} = (0.69 \pm 0.05)M_J$ by Mazeh et al. (2000).

Following the discovery of the short-period planet orbiting 51 Peg (Mayor & Queloz 1995), theoretical models of Jovian-mass planets subject to strong irradiation were computed (Guillot et al. 1996). These models predicted that short-period Jovian planets with effective temperatures of order 1400 K would be significantly larger than Jupiter. The subsequent discovery that HD 209458b has a large radius initially seemed to confirm these models.

While the radius of HD 209458b is certainly broadly consistent with its being a gas giant composed primarily of hydrogen, a study by Guillot & Showman (2002) showed that a standard model of a contracting, irradiated planet can recover $R_{\text{pl}} \sim 1.35R_J$ for HD 209458b only if the deep atmosphere is unrealistically hot. This calculation, as well as more recent work by Bodenheimer et al. (2003) and Chabrier et al. (2004), shows that the predicted radii are $R_{\text{pl}} = (1.1 \pm 0.1)R_J$, significantly outside the 1σ observational uncertainty. The heating effect of the star does increase the predicted radius over that of an isolated planet, but only by about 10%, and not by 30%–40% as observed for HD 209458b.

A number of resolutions to the problem of HD 209458b's large radius have been suggested. Bodenheimer et al. (2001) argue that HD 209458b might be receiving interior tidal heating through ongoing orbital circularization. This hypothesis was refined by Bodenheimer et al. (2003), who computed grids of predicted planetary sizes under a variety of conditions and showed

¹ UCO/Lick Observatory, University of California, Santa Cruz, CA 95064; laughlin@ucolick.org.

² CBA Belgium Observatory, Landen, Belgium.

³ Department of Physics and Astronomy, San Francisco State University, San Francisco, CA 94132.

⁴ Department of Astronomy, University of California, Berkeley, CA 94720.

⁵ Department of Terrestrial Magnetism, Carnegie Institute of Washington, 5241 Broad Branch Road NW, Washington, DC 20015-1305.

that the then current radial velocity data set for HD 209458b was consistent with the presence of an as yet undetected planet capable of providing the requisite eccentricity forcing. The tidal heating hypothesis predicts that HD 209458b is caught up in an anomalous situation and that the majority of hot Jupiter-type planets will have considerably smaller radii than that observed for HD 209458b.

Guillot & Showman (2002) proposed an alternate hypothesis in which strong insolation-driven weather patterns on the planet are envisioned to drive the conversion of kinetic energy into thermal energy at pressures of tens of bars. They explored this idea by modifying their planet evolution code to include a radially adjustable internal energy source term. They found that if kinetic wind energy is being deposited at adiabatic depths with an efficiency of order 1%, then the large observed radius of the planet can be explained. Their hypothesis thus predicts that other transiting planets with similar masses and at similar irradiation levels should be similar in size to HD 209458b.

A third possible explanation for HD 209458b's distended condition was advanced by Burrows et al. (2003), who argued that the effective radius of a hot Jupiter observed in transit is significantly larger than the photospheric radius reported by planet evolution codes. That is, the large effective optical depth of the upper atmosphere viewed obliquely at the planetary limb causes a larger photometric depth than if the planet were simply an opaque sharp-edged sphere. Burrows et al. (2003) calculated that this effect might add $\Delta R \sim 0.1R_J$ to the effective radius of a planet of $M \sim 0.7M_J$. By assuming that the true observed radius of HD 209458 is near the lower edge of the observed error bar at $1.25R_J$, they were able to account for the large size without resorting to an extra source of interior heating. The Burrows et al. (2003) hypothesis therefore predicts that the observed radii of other transiting planets of the same mass should be of order $0.1R_J$ larger than evolutionary models would otherwise predict.

In the standard core accretion paradigm for giant planet formation, as reviewed, for instance, by Lissauer (1993), Jovian planets arise from the collisional agglomeration of solid $M \sim 10 M_\oplus$ cores over a period of several million years followed by rapid ($\tau \sim 10^5$ yr) accretion of hundreds of Earth masses of nebular gas. The competing gravitational instability hypothesis (e.g., Boss 1997, 2004) posits that gas giant planets condense directly from spiral instabilities in protostellar disks on a dynamical timescale of $\tau < 10^3$ yr. Boss (1998) points out that solid particles in the newly formed planet can precipitate to form a core during the initial contraction phase. Only 1% of the matter in the planet is condensible, however, so in a Jovian-mass planet a core, even if it does form, will be much less massive than in the core accretion scenario.

Theoretical models of giant planets (as tabulated, for instance, by Bodenheimer et al. 2003) indicate that the presence or absence of a solid core in a $0.5M_J$ planet heated to a surface temperature of 1500 K leads to a difference in radius of order $0.1R_J$. This difference exceeds the uncertainty to which the planet's radius can potentially be determined for transits of bright parent stars.

In the past year, the detection rate of transiting extrasolar planets has begun to increase, as a number of photometric transit surveys (see Horne 2003 for more discussion) have come fully online. To date, the most prolific project has been the Optical Gravitational Lensing Experiment (OGLE) survey, which has produced four confirmed transiting planets orbiting parent stars with $V \sim 15$ (OGLE-TR-56b; Konacki et al. 2003; OGLE-TR-113b and OGLE-TR-132b; Bouchy et al. 2004;

Moutou et al. 2004; OGLE-TR-111b; Pont et al. 2004). In addition, Alonso et al. (2004) have detected a transiting planet, TrES-1, orbiting a relatively bright ($V = 11.8$) K0 V-type main-sequence star. These new planets are providing an opportunity for comparison with theoretical radius estimates (e.g., Burrows et al. 2004; Chabrier et al. 2004), and indeed, as we show in this paper, we are on the verge of being able to use transiting planets to distinguish whether or not giant planets generally have cores.

The outline of the rest of this article is as follows. In § 2 we report new photometric and spectroscopic observations of TrES-1. These data allow us to obtain both a tighter constraint on the planetary radius, as well as significantly improved physical characteristics of the parent star. In § 3 we compare our theoretical calculations with the observed planetary radius and use these comparisons to constrain the amount of kinetic heating that can be occurring in the planet. We also compare our radius predictions (from Bodenheimer et al. 2003) to the other recently discovered transiting planets. The current census of transiting planets covers a significant range of masses and effective temperatures, and in each case, we find good agreement between our models and the observed radius without recourse to additional sources of energy. Our findings are in agreement with recently published models for OGLE-TR-56b (Burrows et al. 2004; Chabrier et al. 2004), and our new comparisons for OGLE-TR-111b, OGLE-TR-113b, OGLE-TR-132b, and TrES-1 further reinforce the conclusion that HD 209458b is anomalously large. In § 4 we conclude with a discussion of the ramifications that the newly discovered transiting planets have for the currently ongoing photometric transit surveys.

2. FOLLOW-UP SPECTROSCOPY AND PHOTOMETRY FOR TrES-1

The transiting planet TrES-1 discovered by Alonso et al. (2004) presents an excellent opportunity to obtain spectroscopic and photometric follow-up observations that take advantage of the near optimally luminous parent star. That is, the TrES-1 parent star is bright enough to allow very high signal-to-noise ratio spectra and high precision radial velocities on large telescopes such as Keck, yet at $V = 11.8$ it is dim enough to be surrounded (in a ~ 15 minute \times 15 minute field of view) by comparison stars of similar magnitude for high-quality differential photometry using a small telescope. The fact that a small telescope can be used means that we can efficiently draw on a loosely organized worldwide network of photometric observers.⁶

Shortly after the Alonso et al. (2004) discovery announcement, we obtained a template spectrum of TrES-1 using the Keck Hires-R instrument, along with five radial velocity estimates using the iodine cell technique (see Butler et al. 1996). These five velocities are listed in Table 1, along with estimated instrumental errors. We use these radial velocities, along with the velocities, transit-derived period, and central transit ephemeris reported by Alonso et al. (2004), and our stellar mass estimate of $M_* = 0.87 R_\odot$ to obtain an updated mass estimate for the planet, $M_{pl} = (0.729 \pm 0.036)R_J$. The uncertainty is estimated using a bootstrap Monte Carlo procedure (see Press et al. 1992). Our fit to the two radial velocity data sets has three free parameters, namely, the mass and two velocity offsets. The first, $o_1 = 15.13 \text{ m s}^{-1}$, is an offset velocity added to the first TrES-1 radial velocity, v_1 , reported by Alonso et al. (2004; $t = \text{HJD } 2,453,191.770$, $v_1 = 60.4 \pm 12.8 \text{ m s}^{-1}$). The parameter $o_2 = 5.13 \text{ m s}^{-1}$ is an offset velocity added to all eight of the

⁶ See <http://www.transitsearch.org>.

TABLE 1
RADIAL VELOCITY MEASUREMENTS FOR TrES-1

JD – 2,453,000.0	Radial Velocity (m s ⁻¹)	Uncertainty (m s ⁻¹)
237.97925.....	68.32	3.66
238.83933.....	-102.23	3.27
239.77360.....	-24.53	3.25
239.88498.....	10.00	3.11
240.97685.....	70.68	3.73

Alonso et al. (2004) radial velocities; it accommodates the different velocity zero points of the two sets of measurements.

Using the template spectrum, it is straightforward to implement the recently completed SME high-precision spectral analysis pipeline for measuring the physical properties of the stars in the Keck, Lick, and AAT Doppler velocity surveys (Fischer & Valenti 2004). For TrES-1, we confirm that the spectral type of the star is K0 V and obtain physical parameters that are very close to those estimated by Alonso et al. (2004), albeit with improved precision. These parameters are listed in Table 2. Of particular interest is our radius estimate of $R_*/R_\odot = 0.83 \pm 0.03$. This value agrees with the estimated $R_*/R_\odot = 0.85^{+0.10}_{-0.05}$ quoted by Alonso et al. (2004). The uncertainties that we quote in association with our value of R_*/R_\odot are derived by combining several independent estimates of the stellar radius and associated error. The first method comes from comparing the observed spectrum for TrES-1 with other stars in the Valenti & Fischer (2004) compilation that provide close spectral matches and that have known radii. This procedure yields $R_*/R_\odot = 0.83 \pm 0.032$ for TrES-1 based on the six stars, HD 80133, HD 118972, HD 135599, HD 151877, HD 192020, and HD 200968, whose spectra show the best empirical matches to the TrES-1 spectrum. Alternately, however, when one bases the comparison on the derived physical properties, specifically, T_{eff} , $\log g$, and $[\text{Fe}/\text{H}]$, then one finds an estimate of the stellar radius of TrES-1 of $R_*/R_\odot = 0.78 \pm 0.02$. From the TrES-1 spectrum alone, therefore, we can take the union of these two measurements and obtain an estimate of $R_*/R_\odot = 0.81 \pm 0.05$. We retain the full error range of $0.05R_*/R_\odot$ to account for possible systematic error.

An alternate method for estimating R_* involves interpolating from stellar evolutionary tracks, which given our estimates of $\log g = 4.52$, $T_{\text{eff}} = 5214 \pm 23$ K, and metallicity $[\text{Fe}/\text{H}] = 0.001 \pm 0.04$ allow an estimate of the mass, age, and radius of the star using stellar evolutionary models. Interpolating within the tracks of Girardi et al. (2000), we obtain (for $\log g = 4.518$) an age of 4 Gyr, a mass of $M_*/M_\odot = 0.87$, and a radius of $R_*/R_\odot = 0.85$. Interpolation of the Yonsei-Yale models for the input $\log g$, T_{eff} , and $[\text{Fe}/\text{H}]$ gives a radius of $0.84 R_\odot$ for an assumed age of 5 Gyr, in excellent agreement with the Girardi et al. (2000) tracks. We determine the uncertainty in the stellar mass to be roughly $\Delta M = \pm 0.03 M_\odot$, since outside of this range the stellar model predicts stars of significantly different spectral type.

A third, independent method for both estimating the stellar radius and providing a firm lower bound on the star's size can be derived from a Monte Carlo based analysis of our transit photometry. This method is described below and yields $R_*/R_\odot = 0.83$, with a 1σ lower bound of $R_*/R_\odot = 0.80$. Combining all of the estimates (from the stellar spectrum, evolutionary models, and photometric analysis) leads to our adopted value of $R_*/R_\odot = 0.83 \pm 0.03$ listed in Table 2.

TABLE 2
PLANETARY AND STELLAR PROPERTIES FOR TrES-1

Parameter	Value
P (days) ^a	3.0030065 ± 0.000008
T_c (HJD) ^b	2453186.8060 ± 0.0002
Mass (planet) (M_J).....	0.729 ± 0.036
i	$88.2 \pm 1.0^\circ$
R_p (R_J).....	1.08 ± 0.05
Spectrum.....	K0 V
$\log g$	4.52 ± 0.05
$\log L/L_\odot$	-0.32
$V \sin(i)$ (km s ⁻¹).....	1.08 ± 0.3
R/R_\odot	0.83 ± 0.03
M/M_\odot	0.87 ± 0.03
$[\text{Fe}/\text{H}]$	0.001 ± 0.04
T_{eff} (K).....	5214 ± 23
d (pc).....	157 ± 6

^a Period P taken from Alonso et al. (2004).

^b Central transit epoch T_c taken from Alonso et al. (2004).

We obtained photometry of TrES-1 on the nights of 2004 September 1–2 and September 4–5. On both nights, we observed a complete transit using a 0.35 m f/6.3 telescope and an unfiltered SBIG ST-7XME CCD camera.⁷ For both nights, the computed air mass was $\text{sec } z < 1.5$ for the entire transit duration. Data reduction was accomplished using standard differential aperture photometry techniques and employed an ensemble of seven comparison stars. For each of the two nights, we determined a separate photometric baseline by computing the average differential magnitude of all photometric points obtained before and after the transit. Using the known period $P = 3.030065$ days and the known central transit epoch $T_c = \text{HJD } 2,453,186.8060$ reported by Alonso et al. (2004), we then combined the data from the two nights into a folded light curve. These photometric data are shown in Figure 1. Each individual photometric point represents the average of five measurements.

Using a procedure conceptually similar to that described by Brown et al. (2001), we can fit model light curves to the photometric time series. As discussed in Alonso et al. (2004) and also below, the fits to the data are primarily sensitive to the inclination i of the planetary orbit and to the ratio R_p/R_* of the planetary and stellar radii. We adopt a standard stellar limb-darkening relation $I(\mu)/I(1) = 1 - u(1 - \mu)$, where μ is the cosine of the angle between the line of sight and the normal to the local stellar surface. The value of u was obtained by modeling the spectral energy distribution, $U(\lambda)$, from TrES-1 as a 5214 K blackbody and then computing the relative fluxes in the Johnson-Cousins $UBVRJ$ bands by evaluating

$$f_{UBVRJ} = \int_0^\infty U(\lambda)Q(\lambda)F(\lambda) d\lambda$$

for each filter; $F(\lambda)$ is the Gaussian distribution whose width and centroid are fixed such that it approximates a given band's filter function (Binney & Merrifield 1998), while $Q(\lambda)$ is the quantum efficiency of the Kodak KAF-0402ME chip used in the SBIG ST-7XME camera.⁸ The relative fluxes were then

⁷ Further details on the observational equipment, along with CCD images and ASCII files of the reduced photometric data, can be obtained at <http://www.cbabelgium.com>.

⁸ We obtained $Q(\lambda)$ by digitizing the quantum efficiency graph given at http://www.sbig.com/pdf/2002cat_st7xe.pdf.

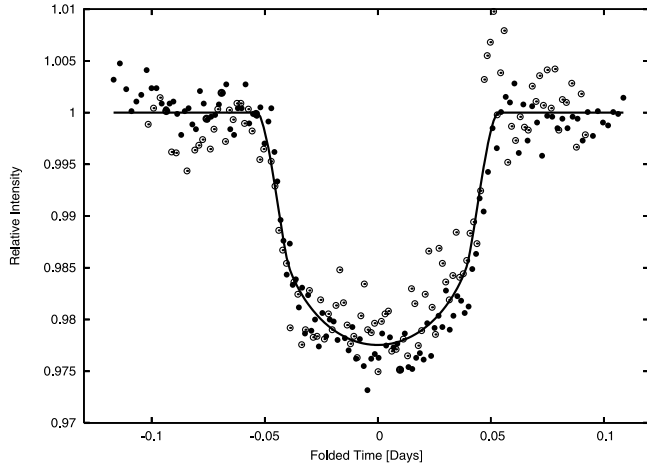


FIG. 1.—Photometric data from combined 2004 September 1 (*filled circles*) and 2004 September 4 (*open circles*) transit observations, with best-fit model light curve.

used to form a weighted average, $u = 0.69186$, of the limb-darkening relations for the *UVBRIJ* bands given by the Claret (2000) model for $[\text{Fe}/\text{H}] = 0.0$, $T_{\text{eff}} = 5250$ K, $\log g = 4.5$, and $v_{\text{mic}} = 1$ km s $^{-1}$. This determination of the limb darkening was used in all of our estimations of the planetary radius.

The stellar mass and radius were initially fixed at the values $M_*/M_\odot = 0.87$ and $R_*/R_\odot = 0.83$ as determined above. For a given choice of these parameters, a light curve is computed by evaluating the fraction of the star's light that is blocked under the assumption that the planet is an opaque disk. We then carried out a two-dimensional grid search for the values of i and R_{pl}/R_* that minimize χ^2 , finding $i = 88^\circ.2$ and $R_{\text{pl}}/R_* = 0.134$. The resulting best-fit light curve is shown overlaying the folded photometry in Figure 1. The uncertainties in i and R_{pl}/R_* stem primarily from two different sources: (1) the observational error in the photometry, and (2) the uncertainty in the stellar radius R_* . Uncertainty in R_{pl}/R_* stemming from photometric error is estimated using a bootstrap Monte Carlo procedure (Press et al. 1992). Individual residuals, σ_i , to the best-fit light curve are sampled (with replacement) and then added back onto the best-fit model to generate alternative realizations of the original data set. Best-fit values for i and R_{pl}/R_* are then evaluated and stored for each of these synthetic data sets. Figure 2 shows the resulting confidence intervals determined assuming $R_*/R_\odot = 0.83$. As the number of synthetic realizations increases, the standard deviation of the calculated result approaches the error due to the observational technique.

Uncertainty in the determination of the stellar radius R_* is found to be the primary source of error in the final estimate of R_{pl} . The photometric depth of the transit depends on the ratio of the cross-sectional areas of the planet and the star, and thus it is expected that to first order, R_{pl}/R_* will remain constant in the face of changes in R_* . The transit width, which depends on R_* , i , and the velocity v_{pl} must also be maintained, but since the flux from the stellar disk is centrally concentrated, changes in i necessitate changes in R_{pl} in order to maintain the observed transit depth. To model this dependence, we calculate best-fit values of R_{pl} for values of R_* within 4σ of the mean. As expected, R_{pl} and R_* are linearly related, with a change in slope at $R_* = 0.80 R_\odot$, corresponding to the onset of fits with central transits. The relation between R_{pl} and R_* is therefore bilinear. For $R_* < 0.8 R_\odot$, increases in i can no longer be used to accommodate the fixed transit duration, and the fits rapidly degrade. As discussed below, the χ^2 statistic of the fits also constrains R_* .

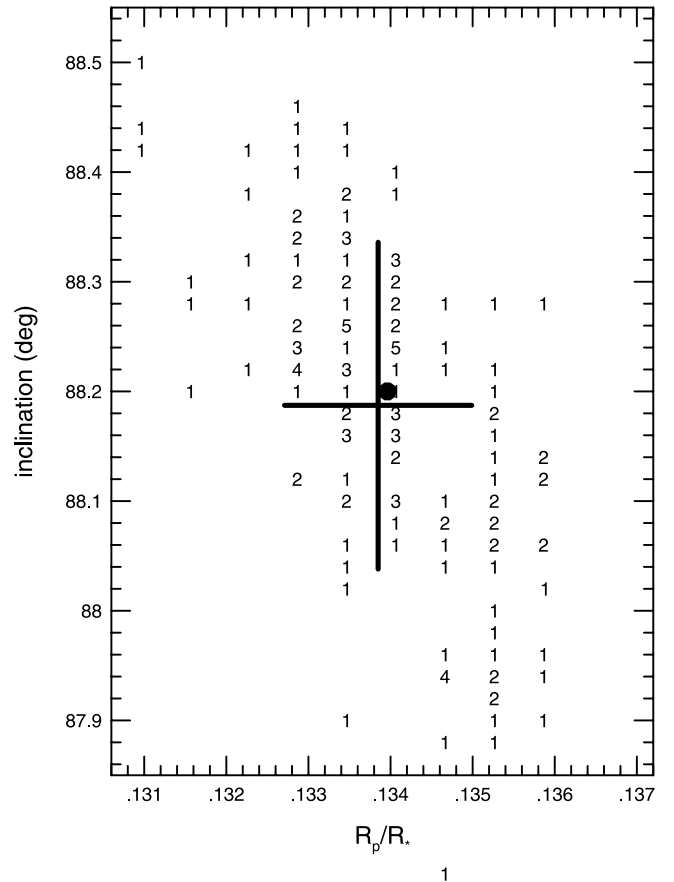


FIG. 2.—Results of a bootstrap Monte Carlo analysis applied to our photometric data. The black dot marks the location of our best-fit inclination, $i = 88^\circ.20$, and radius ratio, $R_p/R_* = 0.1340$, to the combined photometric data set using fixed parameter values $P = 3.030065$ days, $M_* = 0.87 M_\odot$, $R_* = 0.83 R_\odot$, and $T_c = 2,453,186.8060$ (HJD). The numbers report the frequency distribution of outcomes of individual trials of the bootstrap Monte Carlo procedure (see text). The black cross depicts the average result and standard deviation of the Monte Carlo trials, $i_{\text{MC}} = 88^\circ.19 \pm 0^\circ.15$ and $R_p/R_{*\text{MC}} = 0.1338 \pm 0.0011$.

The bootstrap Monte Carlo procedure was repeated for $R_* = 0.79 R_\odot$, $0.82 R_\odot$, $0.85 R_\odot$, and $0.88 R_\odot$. For $R_*/R_\odot > 0.8$, the results of the simulations were found to agree with one another to within 2.4%. For example, for $R_* = 0.82 R_\odot$, we find $R_{\text{pl}}/R_* = 0.1324 \pm 0.0012$, while for $R_* = 0.85 R_\odot$, we find $R_{\text{pl}}/R_* = 0.1338 \pm 0.0011$, and for $R_* = 0.88 R_\odot$, we find $R_{\text{pl}}/R_* = 0.1356 \pm 0.0011$. For the $R_* = 0.79 R_\odot$ case, we find $R_{\text{pl}}/R_* = 0.1323 \pm 0.0008$.

Assuming a normal uncertainty distribution for the stellar radius ($R_* = 0.83 \pm 0.03 R_\odot$), a final Monte Carlo simulation generates values for R_* and finds a corresponding value of R_{pl} based on the bilinear relation between R_{pl} and R_* . The obtained value of R_{pl} is then adjusted by a correction drawn from an average of the Gaussian distributions obtained from the bootstrap procedures performed at $R_* = 0.79 R_\odot$, $0.82 R_\odot$, $0.85 R_\odot$, and $0.88 R_\odot$; 10^5 such trials were accumulated to yield our final estimate of the planetary radius: $R_{\text{pl}} = (1.080 \pm 0.048)R_J$.

Finally, because the TrES-1 occultation comes close to being a central transit, and because the stellar mass estimate of $0.87 \pm 0.03 M_\odot$ is reasonably precise, we can use the photometric transit observations to provide a firm lower bound on the radius of the star. We accomplish this with an additional bootstrap procedure that works as follows. We first take our best fit ($i = 88^\circ.2$, $R_{\text{pl}} = 1.08R_J$, $R_* = 0.83 R_\odot$) to the photometry and create 84 synthetic data sets by drawing with replacement from

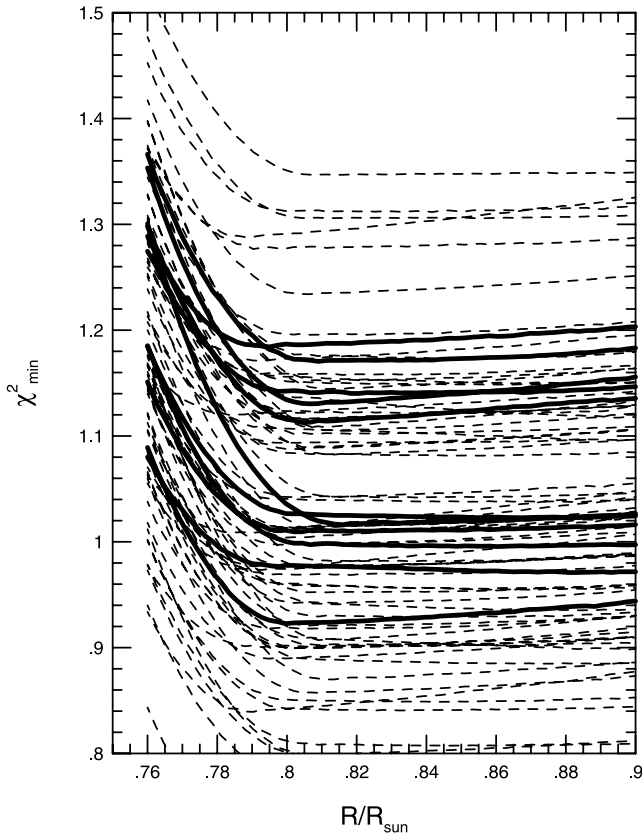


FIG. 3.—Curves of $\chi^2_{\min}(R_*)$ obtained from fits to 84 synthetic data sets obtained using the bootstrap Monte Carlo technique. The sharp increases in χ^2_{\min} as R_* decreases below $0.8 R_{\odot}$ allow for a photometric determination of a lower bound for the radius of the star. Ten of the curves, chosen at random, have been highlighted with heavy dark lines. The remaining curves are shown as light dashed lines.

the scrambled pool of photometric residuals. For each of these synthetic data sets, we then vary our assumption for R_* in increments of $0.01 R_{\odot}$ from $R_* = 0.75$ to $R_* = 0.90 R_{\odot}$. For each guess of R_* , we then perform a full two-dimensional grid search over i and R_{pl} in order to find values for these quantities that minimize the χ^2 of the fit. We then store the run of $\chi^2_{\min}(R_*)$ for each of the 84 synthetic data sets. The resulting $\chi^2_{\min}(R_*)$ curves are plotted in Figure 3. The locations of the minima of these curves can be averaged to give an estimate $R_* = 0.82 R_{\odot}$. Furthermore, the curves are uniformly characterized by a sharp increase in χ^2_{\min} as R_* is decreased below $R_* \sim 0.80 R_{\odot}$, at which point even a central transit cannot account for the observed duration of the photometric dip.

The upper limit on the stellar radius is not well constrained by these $\chi^2_{\min}(R_*)$ curves because decreasing inclination can readily compensate for a larger star. We estimate the 1σ photometric lower bound, $R_{*\text{lower}}$ by equating (if possible) $\chi^2_{\min}(R_{*\text{lower}})$ with $\chi^2_{\min}(0.86 R_{\odot})$ for each curve. (Note that $R_* = 0.86 R_{\odot}$ is the 1σ upper bound on the stellar radius as evaluated by the spectrum, the spectral type, and fits to evolutionary tracks.) We thus derive $R_* = 0.80 R_{\odot}$ as a photometric 1σ lower bound on the radius.

3. MODELS FOR IRRADIATED GIANT PLANETS

Having estimated the radius and mass of TrES-1 as $R_{\text{pl}} = (1.08 \pm 0.05)R_J$ and $M_{\text{pl}} = (0.729 \pm 0.036)M_J$, we are in a position to compare with theoretical evolutionary models. To do this, we use the results of Bodenheimer et al. (2003), who computed sequences of models for insolated planets ranging in

mass from $0.11M_J$ to $3.0M_J$. Separate sequences were computed for models that contained and did not contain solid cores. Sequences of models (again, both with and without cores) were also computed with an energy source term (applied as described by Guillot & Showman 2002) that deposits $\sim 1\%$ of the incoming stellar flux in the regions of the planetary interior, where the pressure is tens of bars. For the purposes of this paper, and to improve interpolation, two new sequences, for $M_{\text{pl}} = 0.75M_J$, were calculated, one with and one without a core of $20 M_{\oplus}$. The physical assumptions in the models are the same as those in Bodenheimer et al. (2003).

Note that these evolutionary sequences use a standard Rosseland mean photospheric boundary condition (eqs. [2] and [3] of Bodenheimer et al. 2003) rather than detailed frequency-dependent atmospheres (Chabrier & Baraffe 2000; Burrows et al. 2003). The opacities that are employed are purely molecular (R. Friedman 2003, private communication) and do not include the possible effects of clouds. The models also assume that the surface temperature is uniform all the way around the planet, even though the rotation of the planet is undoubtedly tidally locked to its orbital motion. Hydrodynamic simulations related to the heating of the night side of the planet have been performed by Cho et al. (2003), Showman & Guillot (2002), and Burkert et al. (2005) under various simplifying assumptions. There is no agreement on what the temperature difference between the day side and the night side of a close-in giant planet should be, and it depends on the assumed opacity in the atmosphere. However, Burkert et al. (2005) suggest that with a reasonable opacity that difference could be in the range 200–300 K, not enough to make an appreciable difference in the radius. The effect on the observationally determined radius caused by the oblique viewing angle, the so-called transit radius effect (see § 1) discussed by Burrows et al. (2003), is not taken into account. Nevertheless, this approximate method gives results that are in agreement with more detailed models (see below), and furthermore, the calculation has been calibrated so that, for the evolution of Jupiter up to the age of 4.5 Gyr, a model with a core gives the correct Jupiter radius to within 1%.

Our results are given in Table 3, where theoretical radii for planets of various masses and equilibrium temperatures are given in the last four columns. The columns labeled “c” and “nc” give the radius, in units of $R_J = 7.1492 \times 10^9$ cm, for models at an age of 4.5 Gyr that include insolation but no additional heating.⁹ The columns labeled “c + kh” and “nc + kh” are the corresponding radii, including the kinetic heating prescription of Guillot & Showman (2002).

For TrES-1, our code predicts $R_{\text{pl}} = 1.05R_J$ for a model with a $20 M_{\oplus}$ core at age 4.5 Gyr. The planetary equilibrium temperature is predicted to be 1011 K. This temperature is derived assuming the stellar properties given in Table 2 and a planetary albedo $A = 0.4$. If the planet has no solid core, then the predicted radius increases to $R_{\text{pl}} = 1.09R_J$. These models both compare well with our size determination of $R_{\text{pl}} = (1.08 \pm 0.05)R_J$, and they suggest that an effective transit radius increase of $\Delta R_{\text{pl}} \sim +0.1R_J$ obtained for HD 209458b by Burrows et al. (2003) may be somewhat smaller in the case of TrES-1, especially if the planet does not contain a core.

Radius predictions for other known transiting planets are shown in Table 3. The radii are obtained by interpolation in Tables 1 and 2 of Bodenheimer et al. (2003). The core mass for models of less than $1.0M_J$ is assumed to be $20 M_{\oplus}$; otherwise, it is assumed to be $40 M_{\oplus}$. These core masses considerably

⁹ Bodenheimer et al. (2003) report planetary radii in units of $R_J = 7.0 \times 10^9$ cm.

TABLE 3
 PREDICTED AND OBSERVED RADII OF IRRADIATED GIANT PLANETS AT $T = 4.5$ Gyr

Planet	Mass (M_J)	T_{eq} (K)	Radius (R_J)	c	nc	c + kh	nc + kh
Jupiter ^a	1.00 ± 0.00	113	$1.00^{+0.00}_{-0.00}$	0.99	1.03	0.99	1.03
OGLE-TR-111b ^b	0.53 ± 0.11	904	$1.00^{+0.13}_{-0.06}$	0.98	1.07	1.19	1.28
TrES-1 ^c	0.73 ± 0.04	1011	$1.08^{+0.05}_{-0.05}$	1.05	1.09	1.14	1.24
OGLE-TR-113b ^d	1.35 ± 0.22	1144	$1.08^{+0.07}_{-0.05}$	1.05	1.09	1.15	1.20
HD 209458b ^e	0.69 ± 0.05	1240	$1.31^{+0.05}_{-0.05}$	1.04	1.09	1.23	1.35
OGLE-TR-56b ^f	1.45 ± 0.23	1686	$1.23^{+0.16}_{-0.16}$	1.09	1.14	1.33	1.40
OGLE-TR-132b ^g	1.19 ± 0.13	1821	$1.13^{+0.08}_{-0.08}$	1.10	1.15	1.37	1.47

^a $R_J = 7.1492 \times 10^9$ cm.

^b M_{pl} and R_{pl} from Pont et al. (2004).

^c M_{pl} and R_{pl} from this paper.

^d M_{pl} and R_{pl} from Bouchy et al. (2004); see also Konacki et al. (2004), who independently find $M_{\text{pl}} = (1.08 \pm 0.28)M_J$ and $R_{\text{pl}} = (1.09 \pm 0.10)R_J$.

^e M_{pl} from Mazeh et al. (2000); R_{pl} from Brown et al. (2001), adjusted by our improved determination of R_* .

^f M_{pl} and R_{pl} from Torres et al. (2004).

^g Observed M_{pl} and R_{pl} from Moutou et al. (2004).

exceed the core masses estimated for Jupiter (0–10 M_{\oplus}) and Saturn (5–15 M_{\oplus}) (e.g., Wuchterl et al. 2000). The overall metal enrichment in Jupiter and Saturn, however, amounts to 30 M_{\oplus} in each object, and previous models show that it is not easy to distinguish between a planet that has a uniformly enriched composition and one that has a solid core surrounded by material of solar composition. Our adopted core masses, therefore, are designed to represent approximately the total excess in heavy elements over solar abundance.

For the case of HD 209458b, the present uncertainty in the measured planetary radius stems largely from the error in the stellar radius. Brown et al. (2001) derive a value $R_* = 1.145 \pm 0.05 R_{\odot}$, based on a combination of stellar models and their photometry. The analysis of Fischer & Valenti (2004) uses high-resolution Keck spectra to produce a set of refined values for the stellar parameters of HD 209458: $T_{\text{eff}} = 6099 \pm 44$ K, $\log g = 4.38 \pm 0.06$, $[\text{Fe}/\text{H}] = 0.014 \pm 0.03$, $v \sin i = 4.5 \pm 0.3$ km s⁻¹, $M_* = 1.11 \pm 0.16 M_{\odot}$, and $R_* = 1.12 \pm 0.05 R_{\odot}$. With this slightly smaller value for R_* , and assuming that R_*/R_{pl} remains constant in the face of small variations in R_* , we estimate a revised observed radius for HD 209458b of $R_{\text{pl}} = (1.32 \pm 0.05)R_J$.

In all cases other than HD 209458b, the models with no kinetic heating provide a good match to the observations. By way of comparison, Burrows et al. (2004) obtain a theoretical radius, without a core, of about $1.2R_J$ for OGLE-TR-56b, in reasonable agreement with our value of $1.14R_J$. Chabrier et al. (2004) obtain a value of about $1.1R_J$, also in agreement with our result and within the observational error bar.

4. DISCUSSION

It is ironic that the first transiting extrasolar planet to be discovered has turned out to be anomalously large; the initial detection of HD 209458b (via the Doppler velocity method) hinged on its mass rather than its radius. From the results in Table 3, we conclude that the (revised) observed planetary size for HD 209458b is about 30% larger than that which will in general be produced by other hot Jupiter-type planets with similar masses and levels of insolation. Many of the existing ground-based transit surveys¹⁰ have designed their detection

thresholds and observational strategies under the assumption that the average short-period transiting planet will have a radius of order $R_{\text{pl}} \sim 1.4R_J$ (as initially indicated for HD 209458b).

The fact that hot Jupiters induce transit depths that are 40%–60% smaller than expected has likely contributed to a significant reduction in yield for ground-based transit surveys. As of 2002, a total of 23 observational efforts reported the combined capability of detecting 2292 planets per year (Horne 2003), whereas the yield to date (2004 October) has comprised only five confirmed planets.

HD 209458b's large radius also makes it easier to interpret a puzzling discrepancy between the statistics of the short-period planets discovered by the transit surveys and by the Doppler velocity methods. Among the 130+ planets detected by the Doppler surveys, the shortest period planets have periods of order 2.5 days (e.g., GJ 436b, $P = 2.644$ days; Butler et al. 2004; HD 73256b, $P = 2.549$ days; Udry et al. 2003), whereas out of the five planets discovered with the transit method, OGLE-TR-56b, OGLE-TR-113b, and OGLE-TR-132b have periods of 1.212, 1.432, and 1.69 days, respectively. Nearly 3000 stars are under radial velocity surveillance, and no detection bias exists against planets with periods of order 1–2 days, so the intrinsic frequency of objects with $P < 1.5$ days is less than $\sim 0.1\%$. We believe that these objects are found preferentially in magnitude-limited transit surveys because they are intrinsically larger ($\bar{R}_{\text{pl}} = 1.2R_J$) than the much more common hot Jupiters with periods of order 3–5 days ($\bar{R}_{\text{pl}} = 1.0R_J$) and hence are easier to detect. The majority of stars in any given transit survey are near the magnitude limit of the survey, at which point a 40% increase in transit depth makes a big difference in terms of detectability. For a discussion of additional biases that affect the relative sensitivities of radial velocity and photometric surveys to short-period planets, see Gaudi et al. (2005).

The statistics of the census of short-period extrasolar planets will be more comprehensible if we can determine the physical mechanism that is responsible for HD 209458b's bloated size. The kinetic heating interpretation of HD 209458b's transit depth is clearly not the primary cause of the inflated radius because it implies a larger than observed size for the newly discovered transiting planets. Furthermore, because HD 209458b and TrES-1b have nearly identical masses and similar effective temperatures, and yet differ in size by $\sim 0.25R_J$, the transit

¹⁰ See the list maintained by Keith Horne at <http://star-www.st-and.ac.uk/~kdh1/transits/table.html>.

radius effect noted by Burrows et al. (2003) cannot fully account for the discrepancy between theory and observation for HD 209458b.

The second companion hypothesis, however, still appears to be a viable interpretation for the large HD 209358b radius. Bodenheimer et al. (2003) showed that a second planet in the HD 209458 system having $M \sim 0.12M_J$, $e \sim 0.4$, and $P \sim 80$ days would gravitationally perturb HD 209458b and maintain a time-averaged eccentricity $\langle e_b \rangle \sim 0.03$. The resulting tidal heating would be sufficient to inflate planet b to its observed radius if the tidal quality factor $Q \approx 2.5 \times 10^5$. In early 2003, the HD 209458 radial velocity data set was consistent with the presence of a perturbing planet of the type studied by Bodenheimer et al. (2003). In early 2004, the best-fit eccentricity to HD 209458b was $e_b = 0.03 \pm 0.016$, suggesting that the orbit of HD 209458b may in fact not be circular. During the present 2004–2005 season, we are carrying out high-cadence monitoring of HD 209458 in order to improve the precision to which e_b is determined, as well as to obtain evidence for a second planet. We also note that by observing the timing of the secondary eclipse, a value of $e \sin \varpi$ can be obtained, thus allowing a measurement of a lower bound on the eccentricity. Both the *MOST* satellite and the *Spitzer* observatory should be capable of observing the secondary eclipse.

In conclusion, we believe that as more transiting planets are detected, it will become possible to make increasingly detailed comparisons with theoretical models. The evolutionary models for giant planets indicate that the planetary radius is sensitively dependent on both the presence or absence of a core and on

the amount of energy that is deposited within the interior of the planet. This dependence is strongest for hot low-mass (i.e., $M < 1M_J$) planets, while being quite weak for planets with large mass (i.e., $M \approx 3M_J$) regardless of the effective surface temperature. The recent discovery of five transiting planets, and in particular the discovery of a planet transiting the relatively bright ($V = 11.8$) star TrES-1, has allowed for accurate radius determinations and for comparison with theoretical radii. These comparisons allow us to draw two immediate conclusions. (1) With the exception of HD 209458b, the transiting extrasolar planets are best fitted by models that include no additional sources of interior heating. (2) HD 209458b likely owes its large radius to a nonzero eccentricity, and this hypothesis will soon be tested.

Just prior to the submission of this paper, a preprint of an article accepted by *Astrophysical Journal Letters* was posted to the Los Alamos preprint server by Sozzetti et al. (2004). Those authors report high-resolution spectroscopic measurements of TrES-1 that yield stellar properties and a planetary radius of $R_{pl} = 1.04^{+0.08}_{-0.05}$ that are in good agreement with the values presented here.

This work was supported by the NASA Origins of Solar Systems Program through grants NNG04GN30G to G. L. and NAG5-13285 to P. B., and by the NASA Terrestrial Planet Finder Precursor Science Program through grant NNG04G191G to G. L.

REFERENCES

- Alonso, R., et al. 2004, *ApJ*, 613, L153
 Binney, J., & Merrifield, M. 1998, *Galactic Astronomy* (Princeton: Princeton Univ. Press)
 Bodenheimer, P., Laughlin, G., & Lin, D. N. C. 2003, *ApJ*, 592, 555
 Bodenheimer, P., Lin, D. N. C., & Mardling, R. A. 2001, *ApJ*, 548, 466
 Boss, A. P. 1997, *Science*, 276, 1836
 ———. 1998, *ApJ*, 503, 923
 ———. 2004, *ApJ*, 610, 456
 Bouchy, F., Pont, F., Santos, N. C., Melo, C., Mayor, M., Queloz, D., & Udry, S. 2004, *A&A*, 421, L13
 Brown, T. M., Charbonneau, D., Gilliland, R. L., Noyes, R. W., & Burrows, A. 2001, *ApJ*, 552, 699
 Burkert, A., Lin, D. N. C., Bodenheimer, P. H., Jones, C. A., & Yorke, H. W. 2005, *ApJ*, 618, 512
 Burrows, A., Hubeny, I., Hubbard, W. B., Sudarsky, D., & Fortney, J. J. 2004, *ApJ*, 610, L53
 Burrows, A., Sudarsky, D., & Hubbard, W. B. 2003, *ApJ*, 594, 545
 Butler, R. P., Marcy, G. W., Williams, E., McCarthy, C., Dossanjh, P., & Vogt, S. S. 1996, *PASP*, 108, 500
 Butler, R. P., Vogt, S. S., Marcy, G. W., Fischer, D. A., Wright, J. T., Henry, G. W., Laughlin, G., & Lissauer, J. 2004, *ApJ*, 617, 580
 Chabrier, G., & Baraffe, I. 2000, *ARA&A*, 38, 337
 Chabrier, G., Barman, T., Baraffe, I., Allard, F., & Hauschildt, P. H. 2004, *ApJ*, 603, L53
 Charbonneau, D., Brown, T. M., Latham, D. W., & Mayor, M. 2000, *ApJ*, 529, L45
 Cho, J. Y.-K., Menou, K., Hansen, B. M. S., & Seager, S. 2003, *ApJ*, 587, L117
 Claret, A. 2000, *A&A*, 363, 1081
 Cody, A. M., & Sasselov, D. D. 2002, *ApJ*, 569, 451
 Fischer, D. A., & Valenti, J. 2004, *ApJ*, submitted
 Gaudi, B. S., Seager, S., & Mollen-Ornelas, G. 2005, *ApJ*, in press
 Girardi, L., Bressan, A., Bertelli, G., & Chiosi, C. 2000, *A&AS*, 141, 371
 Guillot, T., Burrows, A., Hubbard, W. B., Lunine, J. I., & Saumon, D. 1996, *ApJ*, 459, L35
 Guillot, T., & Showman, A. P. 2002, *A&A*, 385, 156
 Henry, G. W., Marcy, G. W., Butler, R. P., & Vogt, S. S. 2000, *ApJ*, 529, L41
 Horne, K. 2003, in *ASP Conf. Ser. 294, Scientific Frontiers in Research on Extrasolar Planets*, ed. D. Deming & S. Seager (San Francisco: ASP), 361
 Konacki, M., Torres, G., Jha, S., & Sasselov, D. 2003, *Nature*, 421, 507
 Konacki, M., et al. 2004, *ApJ*, 609, L37
 Lissauer, J. 1993, *ARA&A*, 31, 129
 Mayor, M., & Queloz, D. 1995, *Nature*, 378, 355
 Mazeh, T., et al. 2000, *ApJ*, 532, L55
 Moutou, C., Pont, F., Bouchy, F., & Mayor, M. 2004, *A&A*, 424, L31
 Pont, F., Bouchy, F., Queloz, D., Santos, N. C., Melo, C., Mayor, M., & Udry, S. 2004, *A&A*, 426, L15
 Press, W. H., Teukolsky, S. A., Vetterling, W. T., & Flannery, B. P. 1992, *Numerical Recipes in FORTRAN: The Art of Scientific Computing* (2nd ed.; Cambridge: Cambridge Univ. Press)
 Showman, A., & Guillot, T. 2002, *A&A*, 385, 166
 Sozzetti, A., et al. 2004, *ApJ*, 616, L167
 Torres, G., Konacki, M., Sasselov, D. D., & Jha, S. 2004, *ApJ*, 609, 1071
 Udry, S., et al. 2003, *A&A*, 407, 679
 Valenti, J., & Fischer, D. A. 2004, *ApJ*, submitted
 Wuchterl, G., Guillot, T., & Lissauer, J. J. 2000, in *Protostars and Planets IV*, ed. V. Mannings, A. P. Boss, & S. S. Russell (Tucson: Univ. Arizona Press), 1081